Ω and ϕ production in a multiphase transport model with enhanced local parton density fluctuation scenario

(Dated: September 4, 2017)

Searching for QCD critical point and mapping the QCD phase diagram are major science goals of the Beam Energy Scan program in Heavy-Ion Collisions. Multi-strange hadron such as Ω and ϕ are important probes for the search of the QCD phase boundaries. The Ω and ϕ are expected to have relatively small hadronic interaction cross sections. Therefore, they can carry the information directly from the chemical freeze-out stage with little or no distortion due to hadronic rescattering. As a result, the production of the Ω and ϕ particle offers a unique advantage in probing the transition from partonic to hadronic dynamics. In this paper, we study the Ω and ϕ production in a multiphase transport model with employment enhanced local parton density fluctuation scenario. We find that the Baryon/Meson ratio is sensitive to the local density fluctuation strength. We also study the flow harmonic of Multi-strange hadron in response to the local density fluctuation.

PACS numbers:

Keywords: multi-strangness particles, AMPT, RHIC

I. INTRODUCTION

Lattice quantum chromodynamics(QCD) calculations suggest that at high temperature and low baryon chemical potential(μ_B), there will be a phase transition from the hadron gas to the quark gluon plasma(QGP), and the phase transition is smooth and continuous. Heavy ion collisions at relativistic energy provide a possibility to study the properties of QGP and QCD phase diagram. The production of multi-strange particles provides a way to investigate the properties of QCD phase diagram.

II. THE AMPT MODEL

A multiphase transport (AMPT) model is a hybrid model to describe heavy ions collisions at relativistic energies [1–4]. It has two versions: default version and string melting version. In our study, we adopt the string melting version to study QCD fluctuation. Because, in string melting version, all the excited strings are converted into partons, it has a clear advantage over the default version in describing the anisotropic flows [5]. The AMPT model consists of four components. The initial stage is described by heavy ion jet interaction generator (HIJING) model [6, 7] that is designed to simulate multiple jets and particle production in heavy ion collisions. Zhang's parton cascade (ZPC) [8] is used to describe scattering among partons, until now, it only includes two-body interaction, but we think it is enough to describe interaction between partons. The hadronization of parton is based on a simple quark coalescence model [3]. The scattering of resulting hadrons is described by a relativistic transport (ART) model [9, 10].

In the transport approach, interactions among partons are described by equations of their Wigner distribution functions, which describe semicalssically their density distribution in phase space. In AMPT model, the total cross section of parton can be described use the following equation [8]

$$\frac{d\sigma_p}{dt} \simeq \frac{9\pi\alpha_s^2}{2(t-\mu^2)^2}, \tag{1}$$

$$\sigma_p \simeq \frac{9\pi\alpha_s^2}{2\mu^2}\frac{1}{1+\mu^2/s}. \tag{2}$$

where α_s is the strong coupling constant and can be a value of 0.47, μ is the screening mass which depend on the medium effect [8], s and t are the usual Mandelstam variables. Using parton scattering cross sections of 6-10 mb, the AMPT model can reproduce the centrality and transverse momentum dependence of hadron elliptic flow [11]. For our study, we take the parton scattering cross section as 10 mb [12]. Until now, for the AMPT program that is being used, it does not contain QCD fluctuation. However, according to the calculation of lattice QCD, the phase transition is smooth and continuous between hadron gas and QGP, this implies that there may be a critical point at the end of the first order phase transition line. Viewed from the thermodynamic, a critical point is a point at which a single thermodynamic state bifurcates into two macroscopically distinct states. This bifurcation may leads to long-ranged thermal fluctuations. To model this effect, a large density fluctuation is introduced at the end of scattering of parton. Shown in Fig. 1 is the distributions of parton in the transverse plane. The upper left is the distribution of parton without QCD fluctuation, the bottom left is the distribution of hadron and final-state hadronic scatterings are closed. Similarly, there are results about QCD fluctuation on the right. it is obvious that the QCD fluctuation of parton can be served in harmonic matter.

III. THE DYNAMICAL COALESCENCE MODEL OF Ω AND ϕ

A dynamical coalescence model has been used to study the production of Ω and ϕ. according to this model, the probability for producing a hadron from partons

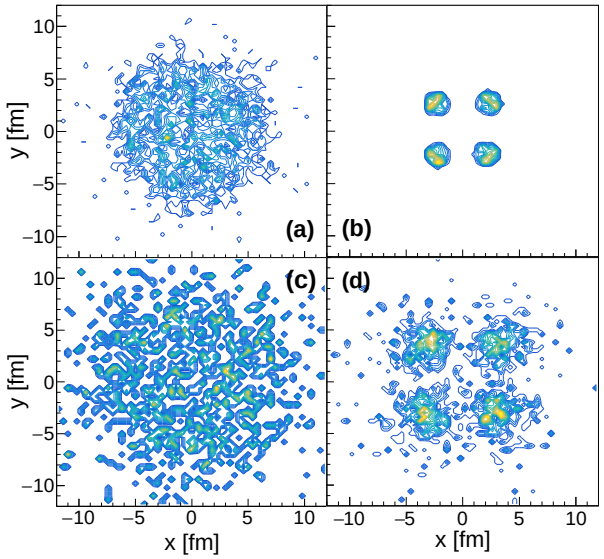

FIG. 1: The distributions of parton and hadron in the transverse plane.

is given by the overlap of parton phase-space distributions with the parton Wigner phase-space function inside hadron [13]. The multiplicity of a M-parton hardon in a heavy-ion collision is given by

$$N_M = G \int d\boldsymbol{r}_{i_1} d\boldsymbol{q}_{i_1} \dots d\boldsymbol{r}_{i_{M-1}} d\boldsymbol{q}_{i_{M-1}} \times \langle \sum_{i_1>i_2>\cdots>i_M} \rho_i^W(\boldsymbol{r}_{i_1}, \boldsymbol{q}_{i_1} \dots \boldsymbol{r}_{i_{M-1}}, \boldsymbol{q}_{i_{M-1}}) \rangle. \quad (3)$$

In Eq. (3), $\langle \dots \rangle$ represents the event averaging; $\mathbf{r}_{i_1},\dots,\mathbf{r}_{i_{M-1}}$ and $\mathbf{q}_{i_1},\dots,\mathbf{q}_{i_{M-1}}$ are the $M-1$ relative coordinates and momenta in the M-parton rest frame; ρ_i^W is the Wigner phase-space function inside the hadron and G is the statistical factor for the M partons.

To determine the quark Wigner phase-space functions inside Ω and ϕ, we need quark wave functions. The quark wave functions can be token as a spherical harmonic oscillator [12]. For the ϕ particle, it can be expressed as

$$\psi(\boldsymbol{r}_1, \boldsymbol{r}_2) = 1/(\pi\sigma_\phi^2)^{3/4}\, exp\left[-r^2/(2\sigma_\phi^2)\right]. \quad (4)$$

where $\boldsymbol{r} = \boldsymbol{r_1} - \boldsymbol{r_2}$ is the relative coordinate and σ_ϕ is a size parameter of ϕ, its normalized wave function leads to a root mean-square radius $R_\phi = (3/8)^{1/2}\sigma_\phi$. The quark Wigner function in ϕ particle can be expressed as

$$\rho_\phi^W(\boldsymbol{r}, \boldsymbol{k}) = 8exp\left(-\frac{r^2}{\sigma_\phi^2} - \sigma_\phi^2 k^2\right). \quad (5)$$

where $\mathbf{k} = (\mathbf{k}_1 - \mathbf{k}_2)/2$ is the relative momentum between s and $\bar{s}$.

Similarly, for Ω^- and $\bar{\Omega}^+$ particles, their wave function can be described by the following equation

$$\psi(\boldsymbol{r}_1, \boldsymbol{r}_2, \boldsymbol{r}_3) = (3\pi^2\sigma_\Omega^4)^{-3/4}\, exp\left(-\frac{\rho^2 + \lambda^2}{2\sigma_\Omega^2}\right). \quad (6)$$

The quark Wigner phase-space function inside the Ω^- and $\bar{\Omega}^+$ baryon can be expressed as

$$\rho_\Omega^W(\rho, \lambda, \boldsymbol{k}_\rho, \boldsymbol{k}_\lambda) = 64\, exp\left(-\frac{\rho^2 + \lambda^2}{\sigma_\Omega^2}\right) exp\left[-(\boldsymbol{k}_\rho^2 + \boldsymbol{k}_\lambda^2)\sigma_\Omega^2\right]. \quad (7)$$

where ρ and λ are relative coordinates of quark, $\mathbf{k}_\rho$ and $\mathbf{k}_\lambda$ are relative momenta, σ_Ω is a size parameter that is related to the root mean-square radius R_Ω.

The two parameters σ_ϕ and σ_Ω in the quark Wigner phasespace functions inside the ϕ meson and Ω baryon are related to their root-mean-square (RMS) radius. we take their values of RMS as $R_\phi = 0.65$ fm and $R_\Omega = 1.2$ fm [12].

IV. TRANSVERSE MOMENTUM SPECTRA OF ϕ AND Ω

Using the parton phase-space information and dynamical coalescence method, we study the effect of QCD fluctuation on transverse-momentum spectra of ϕ and Ω as well as their flow. In Fig. 2, we present the transverse

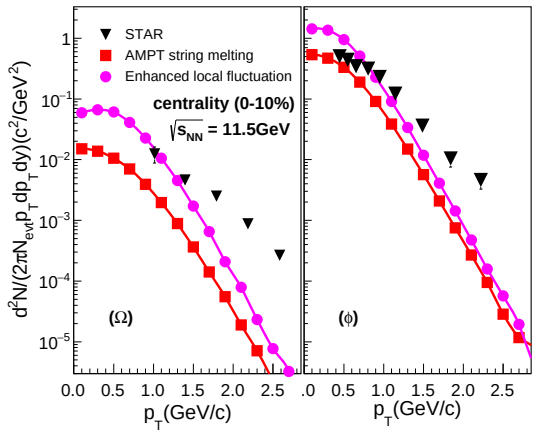

FIG. 2: The transverse momentum spectra: left panel is Ω spectra and right panel is ϕ spectra.

momentum distributions of Ω and ϕ measured at midrapidity ($|y| \lesssim 1$). From these two figures, it is obvious that the QCD fluctuation has the trend to increase the transverse momentum spectra of Ω and ϕ. As a comparison, the experimental data is shown [16]. However, in AMPT, the total number of strange quarks follows the same distribution in different events, in other words, through dynamical coalescence method, the total number of "strange"hadron times the valence quarks number should satisfy the same distribution. So the transverse momentum spectra can not directly response the QCD fluctuation.

Therefore, we also study the ratio of Ω/ϕ as a function of p_t. The result is presented in Fig.3, The measured $N(\Omega^- + \bar{\Omega}^+)/2N(\phi)$ ratio from string melting AMPT is

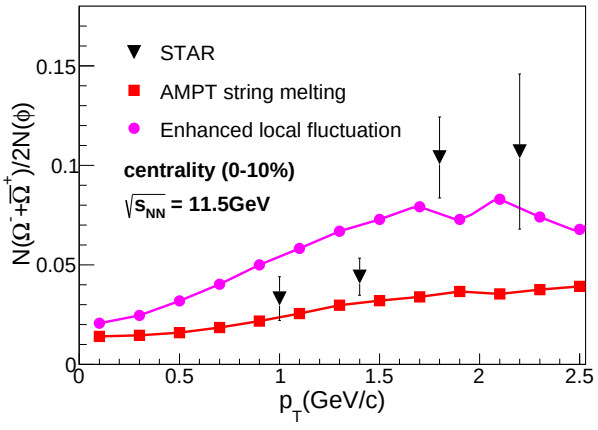

FIG. 3: The ratio of Ω to ϕ.

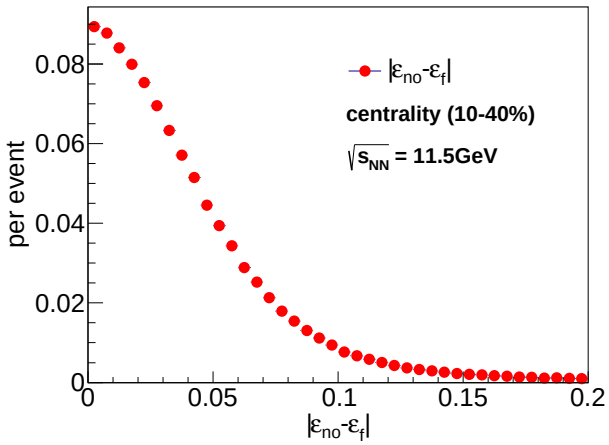

FIG. 4: The result of participant eccentricity.

flat and can describe the experiment data in low p_t, but it underestimates the ratio in high p_t. For the enhanced local fluctuation result, it is obvious that QCD fluctuation has the trend to increase the ratio of Ω to ϕ.

V. ANISOTROPIC FLOWS OF ϕ AND Ω

In this section, we evaluate the effects of variations in the parton density distributions and discuss its effect on elliptic flow. The participant eccentricity ε_{part} can be defined as

$$\varepsilon_{part} = \frac{\sqrt{(\sigma_y^2-\sigma_x^2)^2+4\sigma_{xy}^2}}{\sigma_y^2+\sigma_x^2}. \tag{8}$$

where

$$\sigma_x^2 = \{x^2\}-\{x\}^2 \tag{9}$$
$$\sigma_y^2 = \{y^2\}-\{y\}^2 \tag{10}$$
$$\sigma_{xy} = \{xy\}-\{x\}\{y\}, \tag{11}$$

and $\{\dots\}$ denotes the average over all participants in one event. The result is shown in Fig.4. it is obvious that QCD fluctuation does not have a greater impact on eccentricity. The collectivity in high-energy heavy-ion collisions can be measured through final particle azimuthal anisotropy. The anisotropy coefficients are generally obtained from Fourier expansion of final particle azimuthal distortion [17]. i.e.,

$$E\frac{d^3N}{d^3p} = \frac{1}{2\pi}\frac{d^2N}{p_T dp_T dy}\left(1+\sum_{i=1}^{N}2v_n cos[n(\phi-\psi_{RP})]\right). \tag{12}$$

where E is the energy of final particle, p_T is the transverse momentum, y is the rapidity, ϕ is the azimuthal angle of particle and ψ_{RP} is the reaction plane angle. The Fourier coefficients $v_n(n=1,2,\dots)$ can be described by the following equation

$$v_n = \langle cos(n[\phi-\psi_{RP}])\rangle. \tag{13}$$

Similarly, the calculation of harmonic flow v_n can be relative to the participant plane angle $\psi_n\{P\}$. For the study of QCD fluctuation, we think this method is more appropriate. The participant plane angle can be defined by the following equation

$$\psi_n\{P\} = \frac{1}{n}\left[arctan\frac{\langle r^2 sin(n\varphi)\rangle}{\langle r^2 cos(n\varphi)\rangle}+\pi\right]. \tag{14}$$

where n is nth-order participant plane, r and φ are the coordinates position and azimuthal angle of parton, the symbol $\langle\dots\rangle$ represents density weighting. In Fig. 5, we

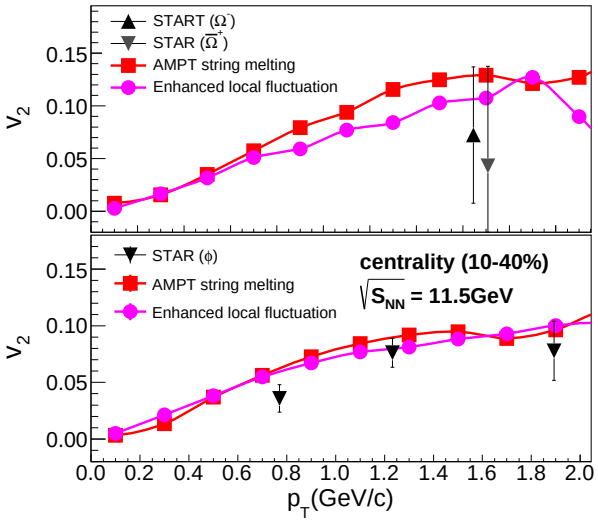

FIG. 5: The elliptic flow: upper panel is Ω flow, bottom panel is ϕ flow.

show the results of v_2. In the range of experiment error, the data from string melting AMPT and enhanced local fluctuation AMPT can be consistent with the experiment. Comparing the two sets of AMPT model data,

the size of v_2 is almost same. because, In AMPT model, the v_2 is mainly developed in the parton cascade stage, moreover, the v_2 of Ω and ϕ is not affected by the hadron interaction due to its small cross-section.

VI. SUMMARY

Based on the parton phase-space information and dynamical coalescence method, we study the effect of QCD fluctuation on the production of Ω baryon and ϕ meson. we have calculated the transverse momentum spectra, ratio and elliptic flow of these particles. For the production of Ω and ϕ, we have found that the QCD fluctuation have the trend to increase the ratio of baryon-to-meson, it can be used as a valid evidence for detecting the QCD critical point. For the v_2 of Ω and ϕ, we have found that it is not sensitive to the QCD fluctuation.

[1] B. Zhang, C. M. Ko, B. A. Li, and Z. W. Lin, Phys. Rev. C **61**, 067901 (2000).
[2] Z. W. Lin, S. Pal, C. M. Ko, B. A. Li, and B. Zhang, Phys. Rev. C **64**, 011902 (2001).
[3] Z. W. Lin, C. M. Ko, B. A. Li, B. Zhang and S. Pal, Phys. Rev. C **72**, 064901 (2005).
[4] B. Zhang, C. M. Ko, B. A. Li, Z. W. Lin, and B. H. Sa, Phys. Rev. C **62**, 054905 (2000).
[5] Y. C. He and Z. W. Lin, arXiv:1703.02673v1 [nucl-th]
[6] X. N. Wang, Phys. Rev. D **43**, 104 (1991)
[7] X. N. Wang, and M. Gyulassy, Phys. Rev. D **44**, 3501 (1991)
[8] B. Zhang, Comput. Phys. Commun. **109**, 193 (1998)
[9] B. A. Li and C. M. Ko, Phys. Rev. C **52**, 2037 (1995).
[10] B. A. Li, A. T. Sustich, B. Zhang, and C. M. Ko, Int. J. Mod. Phys. E **10**, 267 (2001).
[11] Z. W. Lin and C. M. Ko, Phys. Rev. C **65**, 034904 (2002).
[12] L. W. Chen and C. M. Ko, Phys. Rev. C **73**, 044903 (2006).
[13] R. Mattiello, A. Jahns, H. Sorge, H. Stocker and W. Greiner Phys. Rev. Lett. **74**, 2180 (1995).
[14] L. W. Chen, C. M. Ko and B. A. Li, Phys. Rev. C **68**, 017601, (2003).
[15] S. Zhang, J. H. Chen, H. Crawford, D. Keane, Y. G. Ma and Z. B. Xu Phys. Lett. **B684**, 224 (2010).
[16] L. Adamczyk el al. (STAR Collaboration), Phys. Rev. C **93**, 021903(R) (2016).
[17] L. Ma, G. L. Ma and Y. G. Ma, Phys. Rev. C **89**, 044907 (2014).